CHAPTER 6

Chemical epigenetics to assess the role of HDAC1-3 inhibition in macrophage pro-inflammatory gene expression

Maria E. Ourailidou,[a] Niek G. J. Leus,[a] Kim Krist,[a] Alessia Lenoci,[b] Antonello Mai,[b,c] Frank J. Dekker[a]

Manuscript in preparation

[a]Department of Chemical and Pharmaceutical Biology, Groningen Research Institute of Pharmacy, University of Groningen, Antonius Deusinglaan 1, Groningen 9713 AV, The Netherlands
[b]Department of Drug Chemistry and Technologies, 'Sapienza' University, 00185 Rome, Italy
[c]Pasteur Institute, Cenci Bolognetti Foundation, 'Sapienza' University, 00185 Rome, Italy

Abstract

Histone deacetylases (HDACs) have been used as a pharmacological target for the treatment of various diseases. Some non-selective HDAC inhibitors (HDACi) have been clinically-used as therapeutic agents for treatment of hematological cancers but their cytotoxic side effects are an important downside. The discovery of more selective inhibitors has certified the involvement of individual HDACs in pathological processes but the elucidation of the role of specific isoforms in inflammatory responses still remains a challenge. Here, we report the development of closely related, structural analogues of the clinically-used HDACi Entinostat *via* a chemical epigenetic approach. Three compounds were designed and synthesized in which the lid moiety of Entinostat was replaced by an azobenzene group that is either *para*, *meta* or *ortho* substituted to change the selectivity profile among HDACs 1-3. Next, these inhibitors were evaluated for selectivity towards these isoforms and their effect on pro-inflammatory gene expression in macrophages. One analogue, compound **4**, lacked selectivity among HDACs 1-3 and demonstrated inhibition of NF-κB reporter gene activity and pro-inflammatory gene expression in RAW264.7 macrophages.

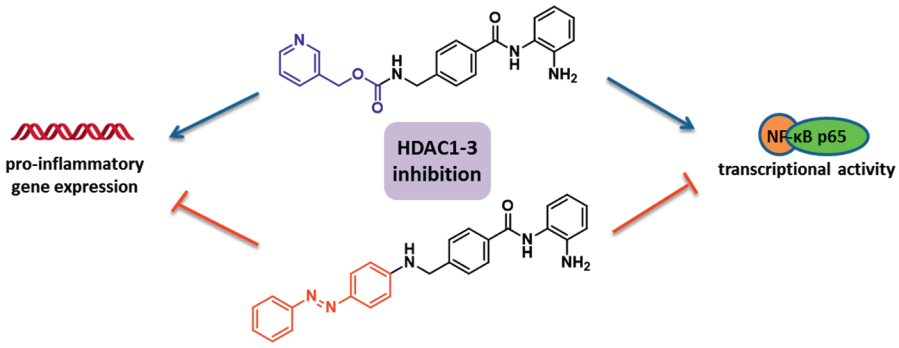

Introduction

Reversible lysine acetylation has been extensively proven to play a critical role in epigenetic regulation of gene expression.[1–5] Lysine acetylation is catalyzed by histone acetyltransferases (HATs) (writers), leading to transcriptionally active chromatin, while the reverse process is catalyzed by histone deacetylases (HDACs) (erasers) resulting in condensed chromatin and transcriptional silencing. Over the past decades, eighteen mammalian HDACs have been identified and divided into four classes (I-IV), according to their sequence homology to yeast orthologs.[6] Among them, class I, containing the zinc-dependent HDACs 1-3 and 8, is crucial for normal cell survival, homeostasis, proliferation and gene expression.[7] Consequently, mounting evidence points to a link between abnormal HDAC activity and inflammatory,[8] neurological diseases,[9] tumorigenesis,[9,10] and metabolic disorders.[11]

There is a tremendously increasing interest in the development of HDAC inhibitors (HDACi) as potential therapeutic agents for several pathological conditions. To date, a wide variety of small molecules has been reported to target HDACs, with differences in their structure, potency, selectivity and, thus, pharmacological effects.[7,12] However, a limited number has reached clinical trials and has been approved for medical use, mainly for treatment of cancer patients.[13,14] The lack of specificity over HDAC classes or isoforms and their subsequent side effects hamper their further applications. Recently, significant efforts in the field of medicinal chemistry have led to the discovery of more selective inhibitors[9,15–20] that have shed some light on the role of individual HDACs in specific diseases. Yet, the important question that remains to be answered is whether inhibition of specific isoforms, in an attempt to improve the therapeutic window, will be actually beneficial in terms of both safety and efficacy. In order to address this issue it is imperative to develop novel methods to investigate the inhibition pattern needed for each disease model.

Our interest lies in the better understanding of the role of class I HDACs in inflammatory signaling. It is known that HDACs influence the activation of NF-κB pathway, a key mediator in inflammatory diseases like COPD and asthma.[21,22] Studies indicate that acetylations of specific lysine residues of NF-κB p65 transcription factor affect its transcriptional capacity, duration of action and DNA binding.[21,23] The alterations observed in NF-κB-mediated gene expression after treatment with HDACi confirms a deacetylation-dependent mechanism of activation.[24–26] Several groups have reported the pivotal role of HDACs 1-3 isoforms in inflammatory responses, such as Schwann cell myelination, intestinal epithelial cell homeostasis and allergic reaction.[27–31] Recently, we explored the function of HDACs 1-3 in inflammatory gene expression in LPS/IFNγ-stimulated murine macrophages by si-RNA-mediated downregulation.[25] Our data suggested a pro-inflammatory role for HDAC1 and 3. Furthermore, selective pharmacological HDAC3 inhibition by RGFP966 demonstrated an attenuation of pro-inflammatory signals in models for inflammatory lung diseases. Yet, further optimization is required in the development of novel HDACi, mainly against HDAC1 and 3, as anti-

inflammatory therapeutics in order to obtain a clearer picture on which HDAC isoform to target.

A very promising approach towards this aim is the use of chemical epigenetic tools, where a parental clinically available agent is slightly modified to generate closely related inhibitors with a different selectivity profile among biological isoforms. This approach aims at the fine-tuning of the isoform selectivity of inhibitors with respect to their pharmacological effects.[32] Therefore, we set out to design closely related analogues of Entinostat (MS-275), an *ortho*-aminoanilide containing HDAC1-3 inhibitor with proven therapeutic properties, currently undergoing clinical trials for treatment of various cancers.[33] These analogues embody isomeric *ortho*-aminoanilide-type HDAC inhibitors with an azobenzene lid. Inhibition and kinetic studies against class I HDACs were performed in order to evaluate their potency and binding kinetic parameters. Next, we tested the effects of the inhibitors on transcriptional activity and intracellular localization of NF-κB p65 as well as inflammatory gene expression in LPS/IFNγ-stimulated murine macrophages. Interestingly, one analogue (compound **4**, *para* isomer) demonstrated remarkably improved anti-inflammatory characteristics compared to Entinostat providing insight in the selectivity profile required to attenuate macrophage-mediated pro-inflammatory responses.

Results and discussion

Chemical epigenetic design. For our purposes, we chose Entinostat as a starting point to design novel HDAC1-3 inhibitors with refined characteristics. The *ortho*-aminoanilide group, that serves for zinc binding, is advantageous compared to the hydroxamic acid moiety (like Suberanilohydroxamic acid, SAHA, pan-HDACi) as it assures for selective inhibition among class I HDACs 1-3, reducing cytotoxicity.[34–36] Our modifications were limited to the cap region of Entinostat, where an azobenzene group was introduced to a *para*, *meta* and *ortho* position with respect to the amine group of the connection unit of the parental inhibitor (compounds **4**, **7**, and **9** respectively, Figure 1A). Azobenzenes are often used in photopharmacology as photoswitches that allow for two isomeric forms, preferably the *cis* being more active than the *trans*.[37,38] Previously, we developed successfully SAHA photoswitchable derivatives as potential antitumor agents.[39] Our data demonstrated that substitution of the cap of the original drug with an azobenzene group in the *para*, *meta* and *ortho* position led to notable differences in terms of potency of the *trans* form (*meta* and *ortho* isomers more active than *para*). This encouraged us to employ the same structural alterations in Entinostat in an attempt to improve potency and specificity over HDACs 1-3 and gain more information on the selectivity profile required to inhibit pro-inflammatory gene expression in macrophages.

Synthesis. The starting materials were synthesized as described previously.[39] Two synthetic routes were followed for the production of the Entinostat analogues (see Supplementary information). Compound **4** was synthesized by a reductive amination reaction between methyl-4-formylbenzoate and (*E*)-4-(phenyldiazenyl)

aniline. Subsequent hydrolysis to the corresponding ester allowed for coupling to the mono Boc-protected 2-aminoaniline. Boc deprotection using a solution of 4N HCl afforded compound **4**. As for compounds **7** and **9**, the peptide coupling between the mono Boc-protected 2-aminoaniline and 4-formylbenzoic acid was performed first followed by reductive amination using the corresponding (phenyldiazenyl)aniline. For compound **7**, the deprotection of Boc group was performed as for compound **4**, while the same conditions led to benzyl cleavage due the basic nature of the amino group at the *ortho* position of the azobenzene in compound **9**. In this case, milder acidic conditions were used by employing trifluoroacetic acid.

K_i values reveal no selectivity among HDAC1-3. The resulting collection of structurally-related HDACi was tested for HDAC inhibition *via* an assay based on the measurement of the deacetylation of a pro-fluorogenic substrate.[39] Prior to testing, the stock solutions of the inhibitors (10 mM in DMSO) were heated at 60 °C for 10 min to ensure occurrence of the azobenzene in its *trans* isomeric form. Various concentrations of each inhibitor were incubated with HDAC1, 2, 3 or 8 in presence of the substrate Boc-Lys(Ac)-AMC at room temperature. After one hour, the reaction was stopped by the addition of 100 µM of SAHA and trypsin to cleave the deacetylated lysine, resulting in the release of fluorescent 7-amino-4-methylcoumarin (AMC). The IC_{50} values obtained were used to calculate the K_i values by application of the Cheng-Prusoff equation (see Supplementary information). As expected for *ortho*-aminoanilide-type inhibitors, no inhibition was observed against HDAC8. We found that Entinostat inhibits HDAC1-3 activity with Ki values in the low nM range, exhibiting the greatest potency against HDAC1 (120 nM, Table 1). In comparison to the parental agent, the azobenzene lid-carrying compounds **4**, **7** and **9** lost largely their selectivity among HDACs 1-3.

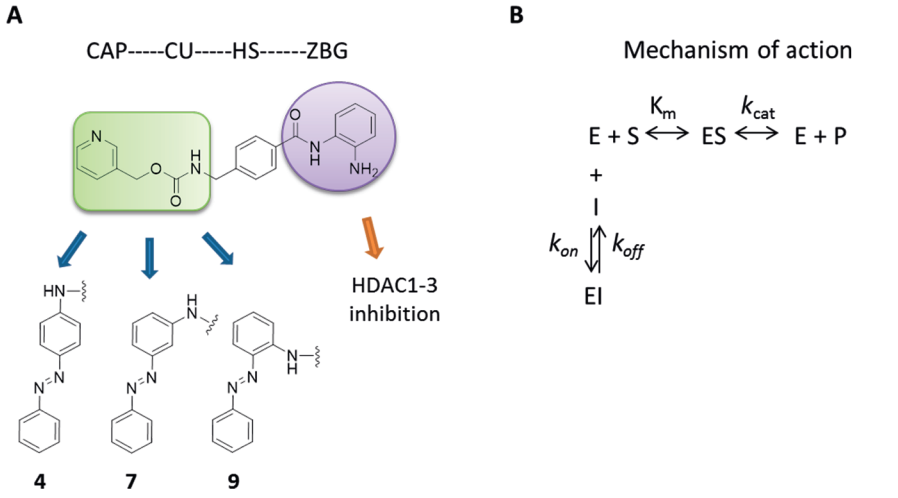

Figure 1. A) Design of structural analogues of Entinostat. An azobenzene moiety was introduced into the CAP region in *para* (**4**), *meta* (**7**) and *ortho* (**9**) position in respect to the amine group of the CU of Entinostat. B) Mechanism of action of slow, tight-binding inhibitors. CU; connection unit, HS; hydrophobic spacer, ZBG; zinc-binding group.

Except for the *meta* isomer that displayed for HDAC1 a potency of 0.63 μM, the K_i values in all the other cases were found to be in the low μM range with no significant difference among individual isoforms. Taken these data together, we speculated that enzyme binding kinetics may potentially be more informative on the selectivity and behavior of the inhibitors inside the biological targets.

Binding kinetic analysis reaffirms a non-isoform-selective profile. There is strong evidence that *ortho*-aminoanilides are slow, tight-binding inhibitors, following the mechanism of enzyme inhibition as shown in Figure 1B.[32,40] In contrast to hydroxamate-based inhibitors, they act *via* a slow on/slow off binding; they are characterized by low association rate constants (k_{on}) and form a tight complex with the enzyme (EI), exhibiting long residence times. In order to determine the kinetic parameters of each inhibitor, Lys-C peptidase was used as a developer instead of trypsin as described by Chou *et al*. to prevent enzyme degradation.[41] Moreover, the deacetylation reaction was not stopped by the addition of SAHA but HDAC activity was monitored over time to generate progress curves allowing for the investigation of the rate constants.[41]

According to a previously reported protocol, the measurement of the association rate constants (k_{on}) involved the incubation of HDACs 1-3 with different concentrations of the inhibitors in presence of Lys-C and high amounts of the substrate ($5xK_M$).[41] The fluorescence was monitored for 60-90 min at room temperature. The progress curves of all the inhibitors confirmed a time-dependent mechanism of HDAC inhibition and a linear relationship between k_{obs} and inhibitor concentration as observed before (k_{on} values were calculated as described in the Supplementary section).[41] Regarding HDAC1, compounds **4** and **7** indicated slightly faster binding rates than Entinostat (1.5 and 1.8× accordingly), whereas the observed k_{on} values in HDAC2 were either similar (**4**) or lower than the ones of Entinostat (Table 1). Considering HDAC3, the same compounds gave comparable results with the parental inhibitor Entinostat, while **9** was found to bind much slower (3.5×).

The off-rate constants (k_{off}) were determined after 100-fold dilution of samples containing high concentrations of HDACs 1-3 pre-incubated for 1h with each inhibitor, and subsequent measurement of HDAC activity as described above (see Supplementary information).[41] The dissociation rate of the enzyme-inhibitor complexes was equivalent for all the inhibitors, with only compound **7** being released faster from HDAC1 and both **7** and **9** exhibiting slightly lower residence in HDAC2 and 3 (Table 1).

In terms of selectivity among isoforms, all the compounds appear to bind faster in HDAC1, less fast in HDAC2 and even slower in HDAC3 (compound **7** presented similar k_{on} values in HDAC2 and 3). A certain pattern was also noticed during dissociation experiments, where we discovered that inhibitors are generally released rapidly from HDAC3, less fast from HDAC1 and remain longer in HDAC2 (compound **7** presented similar k_{off} values in HDAC1 and 3). Comparable results were obtained with the reference Entinostat. Taking into consideration the k_{on} and k_{off} values of the analogues combined, our observations are consistent with the affinity values (K_i) calculated before.

Table 1. Binding affinity and kinetic rate constants of Entinostat and its *para* (**4**), *meta* (**7**) and *ortho* (**9**) azobenzene analogues against HDACs 1-3. The values are presented as mean values of three independent measurements with their respective standard deviations.

	K_i (μM)			k_{on} ($\cdot 10^6$ min^{-1} M^{-1})			k_{off} (min^{-1})		
Compound	**HDAC1**	**HDAC2**	**HDAC3**	**HDAC1**	**HDAC2**	**HDAC3**	**HDAC1**	**HDAC2**	**HDAC3**
Entinostat	0.12±0.03	0.23±0.05	0.60±0.12	0.092±0.008	0.102±0.015	0.059±0.003	0.076±0.006	0.034±0.002	0.098±0.005
4	1.8±0.13	1.8±0.16	1.3±0.23	0.137±0.019	0.073±0.003	0.043±0.005	0.067±0.007	0.046±0.008	0.103±0.01
7	0.63±0.04	2.4±0.3	1.4±0.13	0.166±0.008	0.048±0.001	0.055±0.002	0.162±0.013	0.061±0.003	0.139±0.01
9	1.7±0.2	3.9±0.4	2.6±0.4	0.066±0.002	0.039±0.003	0.017±0.001	0.104±0.006	0.064±0.003	0.148±0.012

Compound 4 exhibits anti-inflammatory effects in LPS/IFNγ-stimulated murine macrophages. Extensive literature has established the connection between HDACs 1-3 and inflammatory signaling in macrophages.[42–44] In order to investigate the effect of *para*, *meta* and *ortho* azobenzene analogues of Entinostat in inflammatory pathways *via* HDAC inhibition, we performed a series of pharmacological studies in RAW264.7 murine macrophages. Each time, cells were incubated with the respective inhibitor for 20h followed by inflammatory stimulation with LPS and IFNγ during the last 4h to ensure activation towards M1 (pro-inflammatory) macrophages.

First, we explored the cell viability after treatment with different concentrations of HDACi. Importantly, compounds **4**, **7** and **9** showed no effect on cell viability at concentrations up to 50 μM (see Supplementary information), whereas Entinostat was found to be toxic at concentrations higher than 2.5 μM. Next to this, the stability of the azobenzene-containing inhibitors towards reduction in cellular environment was previously verified after testing in presence of 10 mM of glutathione.[39]

Compound 4 attenuates NF-κB p65 transcriptional activity. Upon stimulation (e.g. by inflammatory cytokines), the p50-p65 heterodimer is released from the complex with IκBα and translocated to the nucleus, resulting in the upregulation of the expression of specific genes.[21] As mentioned in the introduction, acetylation and, consequently, deacetylation are of key importance in the regulation of NF-κB p65 transcriptional activity. The latter was assessed using a reporter gene assay (see Supplementary information). RAW264.7 cells were treated with compounds

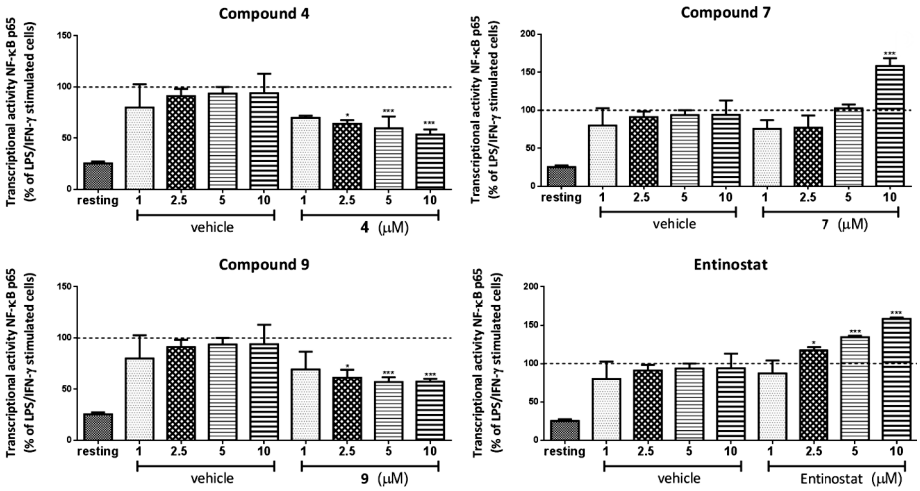

Figure 2. Effects of Entinostat and its *para* (**4**), *meta* (**7**) and *ortho* (**9**) azobenzene analogues on LPS/IFNγ-induced NF-κB p65 transcriptional activity. RAW blue cells were treated with the respective HDAC inhibitors at the indicated concentrations for 20h and stimulated with LPS/IFNγ for the last 4h of the experiment. Data are shown as representative data set of 3 independent experiments with the respective ± SD. * $p < 0.05$, *** $p < 0.001$ compared to vehicle-treated group.

4, **7** and **9** in a concentration range 1-10 μM. Interestingly, treatment with *para* (**4**) or *ortho* (**9**) isomers resulted in inhibition of NF-κB p65 transcriptional activity with the highest effect observed at 10 μM (up to 50% reduction, Figure 2). On the contrary, a robust activation of NF-κB p65 was found in case of 10 μM of *meta* derivative (**7**), while lower concentrations gave no change. The reference compound Entinostat displayed significant upregulation but only when used at the toxic concentrations of 5 and 10 μM.

These findings provided the first indications that minimal structural modifications and relatively limited changes in inhibitory selectivity among HDACs 1-3 can result in considerable differences in pharmacological performance. The higher potency of Entinostat and compound **7** against HDAC1, compared to **4** and **9**, raises the idea that HDAC1 inhibition plays an essential role in activation of NF-κB p65 and, consequently, in the expression of numerous genes involved in inflammatory processes. This is in line with our previous work that supported that HDAC3-selective inhibition by RGFP966 suppressed NF-κB p65 transcriptional activity.[25]

Compound 4 reduces NF-kB p65 nuclear translocation. Fluorescence microscopy was used to locate NF-κB p65 in the nucleus of LPS/IFNγ-stimulated RAW264.7 macrophages (see Supplementary information). After proper staining, NF-κB p65 was shown in green while cell nuclei were visualized in blue (Figure 3). Immunofluorescence microscopy images were overlaid and compared to vehicle. In our experiments, compound **7**, as Entinostat, presumably enhanced the nuclear translocation of NF-κB p65 (Figure 3). In contrast, compounds **4** and **9** rather reduced p65 nuclear translocation. Collectively, these data are in line with the studies on the NF-κB transcriptional activity that indicated inhibition for compounds **4** and **9** and activation for **7**. Hence, decrease of HDAC1 inhibitory potency implies a reduction of the transcriptional activity and nuclear localization of NF-kB p65.

Compound 4 reduces the expression of pro-inflammatory genes. After cellular LPS/IFNγ-stimulation and treatment with 1, 5 and 10 μM of each Entinostat analogue, we set out to monitor the expression levels of TNFα, iNOS, IL-1β, IL-6 and IL-12b. We were pleased to find that, with the exception of iNOS, compound **4** caused a dose-dependent reduction in the expression of the other pro-inflammatory cytokines while in case of **7** and **9** target genes were either unaffected (IL-1β, IL-12b) or overexpressed (iNOS) (Figure 4). Only regarding TNFα expression, 10 μM of **7** resulted in downregulation and the same effect was observed with compound **4** and subtoxic concentration of the reference Entinostat. Moreover, analogously to Entinostat, compounds **7** and **9**, when used at their highest concentrations, largely induced the expression of iNOS, whereas compound **4** had no influence. Notifying, suppression of IL-1β and IL-12b was demonstrated only after treatment with compound **4** in contrast to the phenomenal increase produced by the reference Entinostat. At last, all analogues appeared to limit the expression of IL-6 in a concentration-dependent manner with the most remarkable results coming from compound **4** (90% inhibition at 10 μM). Favorably, these data clarify a pronounced anti-inflammatory profile for the *para* isomer **4** and suggest that inhibition should

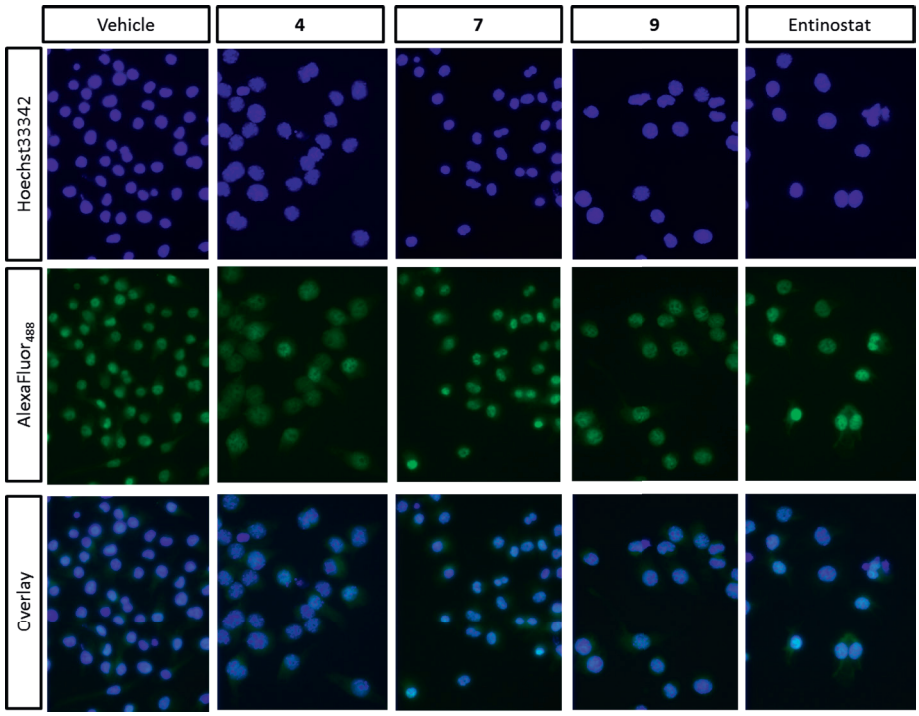

Figure 3. Effects of Entinostat and its *para* (**4**), *meta* (**7**) and *ortho* (**9**) azobenzene analogues on nuclear translocation profile of NF-kB p65 in RAW264.7 macrophages. After 20h incubation with 1 µM of the respective inhibitors followed by 1h LPS/IFNγ stimulation, RAW264.7 macrophages were prepared for immunofluorescence microscopy. Green signal represents NF-kB p65 protein, while the blue signal visualizes the Hoechst stained nuclei.

be maintained over the HDAC 1, 2 and 3 isoforms in order to attenuate the overall expression of pro-inflammatory cytokines in macrophages. Furthermore, the fact that Entinostat and compound **7** promoted greatly the expression of iNOS shows that HDAC1 inhibition is associated to the upregulation of this gene suggesting a pro-inflammatory effect when HDAC1 activity is suppressed.

Surprisingly, opposed to the significant induction of the mRNA levels of the anti-inflammatory cytokine IL-10 caused by Entinostat, none of its azobenzene analogues had an obvious influence on its expression (Figure 4). This indicates that the pyridine-containing lid of Entinostat seems to be crucial for the upregulation of IL-10, which is connected to a potential anti-inflammatory effect of Entinostat.

Conclusions

There is solid evidence that class I HDACs are of great importance in pro-inflammatory gene expression *via*, among others, the NF-kB pathway. While some pan-HDACi have been proven to be effective in the treatment of inflammatory

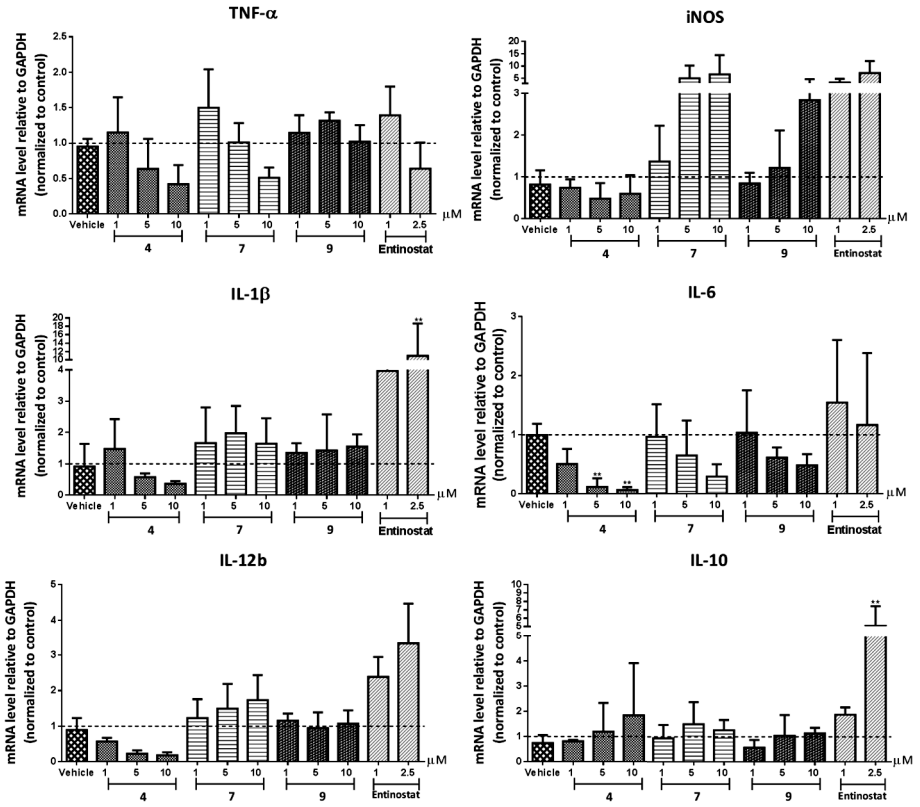

Figure 4. Effects of Entinostat and its *para* (**4**), *meta* (**7**) and *ortho* (**9**) azobenzene analogues on pro- and anti-inflammatory gene expression in RAW264.7 macrophages. Cells were treated with the respective HDAC inhibitors at the indicated concentrations for 20h and stimulated with LPS/IFNγ for the last 4h of the experiment. Gene expression was analyzed by RT-q-PCR. For vehicle treatment, cells were pre-treated with a proportional dilution of the inhibitor solvent DMSO. Data represent the target gene expression normalized to the reference gene. Data are presented as mean values ± SD of 3-4 independent experiments. ** $p<0.01$ compared to vehicle-treated group.

diseases, they usually suffer from cytotoxicity that limits their therapeutic applications. Moreover, their divergent effects on inflammatory gene expression have called for the development of isoform-selective HDACi.[44] In this study, we applied a chemical epigenetic strategy to employ structural analogues of a clinically-used agent with small differences in their HDAC inhibitory profile. As a starting point, we selected the *ortho*-aminoanilide-type HDAC1-3 inhibitor Entinostat to generate three derivatives (*para* (**4**), *meta* (**7**) and *ortho* (**9**)) that consist of an azobenzene group as a cap moiety. Compounds were characterized and evaluated for their anti-inflammatory effects aiming at finding the right isoform to target so that such inhibition could ultimately lead to the proper therapeutic behavior.

Firstly, apart from the *meta* isomer that showed a certain preference for HDAC1, further inhibition assays did not reveal an apparent profile of selectivity while potency was reduced compared to the original agent Entinostat. As a next step, the kinetic parameters of each HDACi were determined and confirmed the slow, tight binding mechanism described for all *ortho*-aminoanilide-type inhibitors. We then considered this structurally similar set of inhibitors with slight differences in activity against HDACs 1-3 as a toolbox to explore which HDAC isoform to target in order to inhibit pro-inflammatory gene transcription.

We set out to examine the pharmacological effects of the described HDACi on LPS/IFNγ-induced inflammatory responses in RAW264.7 murine macrophages. Cell viability assays showed that all developed compounds were found to be less toxic than Entinostat. In addition, compounds **4** and **9** appeared to impair NF-κB p65 transcriptional activity and suppress NF-κB p65 nuclear translocation, while **7**, as Entinostat, led to upregulation. These findings suggest that HDAC1 inhibition plays a role in transcriptional activation of NF-κB p65.

Further investigations of the impact of the Entinostat analogues on the expression of pro-inflammatory genes corroborated the anti-inflammatory profile of compound **4**. More specifically, the latter suppressed the production of TNFα, IL-1β, IL-6 and IL-12b in a dose-dependent way with IL-6 expression being almost depleted at 10 μM. On the other hand, compound **9** induced iNOS and decreased IL-6 mRNA levels, while other genes were unaltered. Lastly, compound **7** reduced TNFα and IL-6 expression and exhibited the same remarkable effects with Entinostat on the activation of iNOS expression. These data support the hypothesis that a non-selective profile over HDACs 1-3 is needed to achieve the desirable anti-inflammatory effects.

Regarding the expression of the anti-inflammatory cytokine IL-10, in contrast to the significant increase triggered by Entinostat, no apparent changes were noticed after treatment with the azobenzene analogues. This implies that strong HDAC1 and HDAC2 inhibition is tightly linked to IL-10 upregulation, which can be lost with modifications on the cap of Entinostat.

In conclusion, the improved anti-inflammatory characteristics of compound **4** compared to Entinostat demonstrate that a non-selective inhibition of HDACs 1-3 offers a promising potential. This sets the stage for further development and exploration of the contribution of HDAC1, 2 and 3 in drug discovery effort aimed at the development of anti-inflammatory therapeutics.

Contributions

The synthesis, inhibition, kinetic studies and writing of the manuscript were performed by M. E. Ourailidou. A. Lenoci contributed to the synthesis of the compounds. N. G. J. Leus and K. Krist performed the pharmacological experiments. Supervision of the project was done by F. J. Dekker and A. Mai. All authors contributed in the revision of the manuscript.

Acknowledgements

This work was financially supported by a VIDI grant (723.012.005) from the Netherlands Organization for Scientific Research and an ERC starting grant (309782) from the European Union to F. J. D. We also acknowledge W. Szymanski for providing the starting materials for the synthesis of the reported compounds.

References

1. Mizzen, C. A., and Allis, C. D. (1998) Linking histone acetylation to transcriptional regulation. *Cell. Mol. Life Sci. 54*, 6-20.
2. Turner, B. M. (2000) Histone acetylation and an epigenetic code. *BioEssays 22*, 836-845.
3. Grunstein, M. (1997) Histone acetylation in chromatin structure and transcription. *Nature 389*, 349-352.
4. Delcuve, G. P., Khan, D. H., and Davie, J. R. (2012) Roles of histone deacetylases in epigenetic regulation: emerging paradigms from studies with inhibitors. *Clin. Epigenetics 4*, 5.
5. Cameron, E. E., Bachman, K. E., Myöhänen, S., Herman, J. G., and Baylin, S. B. (1999) Synergy of demethylation and histone deacetylase inhibition in the re-expression of genes silenced in cancer. *Nat. Genet. 21*, 103-107.
6. Gregoretti, I. V., Lee, Y. M., and Goodson, H. V. (2004) Molecular evolution of the histone deacetylase family: Functional implications of phylogenetic analysis. *J. Mol. Biol. 338*, 17-31.
7. Dokmanovic, M., Clarke, C., and Marks, P. A. (2007) Histone deacetylase inhibitors: overview and perspectives. *Mol. Cancer Res. 5*, 981-989.
8. Shakespear, M. R., Halili, M. A., Irvine, K. M., Fairlie, D. P., and Sweet, M. J. (2011) Histone deacetylases as regulators of inflammation and immunity. *Trends Immunol. 32*, 335-343.
9. Falkenberg, K. J., and Johnstone, R. W. (2014) Histone deacetylases and their inhibitors in cancer, neurological diseases and immune disorders. *Nat. Rev. Drug Discov. 13*, 673-691.
10. Ropero, S., and Esteller, M. (2007) The role of histone deacetylases (HDACs) in human cancer. *Mol. Oncol. 1*, 19-25.
11. Sangshetti, J. N., Sakle, N. S., Dehghan, M. H., and Shinde, D. B. (2013) Histone deacetylases as targets for multiple diseases. *Mini Rev. Med. Chem. 13*, 1005–1026.
12. Minucci, S., and Pelicci, P. G. (2006) Histone deacetylase inhibitors and the promise of epigenetic (and more) treatments for cancer. *Nat. Rev. Cancer 6*, 38-51.
13. Mottamal, M., Zheng, S., Huang, T. L., and Wang, G. (2015) Histone deacetylase inhibitors in clinical studies as templates for new anticancer agents. *Molecules 20*, 3898-3941.
14. West, A. C., and Johnstone, R. W. (2014) New and emerging HDAC inhibitors for cancer treatment. *J. Clin. Invest. 124*, 30-39.
15. Bieliauskas, A. V, and Pflum, M. K. (2008) Isoform-selective histone deacetylase inhibitors. *Chem. Soc. Rev. 37*, 1402-1413.
16. McKinsey, T. A. (2011) Isoform-selective HDAC inhibitors: Closing in on translational medicine for the heart. *J. Mol. Cell. Cardiol. 51*, 491-496.
17. Fournel, M., Bonfils, C., Hou, Y., Yan, P. T., Trachy-Bourget, M.-C., Kalita, A., Liu, J., Lu, A.-H., Zhou, N. Z., Robert, M.-F., Gillespie, J., Wang, J. J., Ste-Croix, H., Rahil, J., Lefebvre, S., Moradei, O., Delorme, D., Macleod, A. R., Besterman, J. M., and Li, Z. (2008) MGCD0103, a novel isotype-selective histone deacetylase inhibitor, has broad spectrum antitumor activity

in vitro and in vivo. *Mol. Cancer Ther. 7*, 759-768.
18. Park, J. H., Jung, Y., Kim, T. Y., Kim, S. G., Jong, H. S., Lee, J. W., Kim, D. K., Lee, J. S., Kim, N. K., Kim, T. Y., and Bang, Y. J. (2004) Class I histone deacetylase-selective novel synthetic inhibitors potently inhibit human tumor proliferation. *Clin. Cancer Res. 10*, 5271-5281.
19. Lee, J. H., Mahendran, A., Yao, Y., Ngo, L., Venta-Perez, G., Choy, M. L., Kim, N., Ham, W.-S., Breslow, R., and Marks, P. A. (2013) Development of a histone deacetylase 6 inhibitor and its biological effects. *Proc. Natl. Acad. Sci. U. S. A. 110*, 15704-15709.
20. Gupta, P., Reid, R. C., Iyer, A., Sweet, M. J., and Fairlie, D. P. (2012) Towards isozyme-selective HDAC inhibitors for interrogating disease. *Curr. Top. Med. Chem. 12*, 1479-1499.
21. Ghizzoni, M., Haisma, H. J., Maarsingh, H., and Dekker, F. J. (2011) Histone acetyltransferases are crucial regulators in NF-κB mediated inflammation. *Drug Discov. Today 16*, 504-511.
22. Dekker, F. J., van den Bosch, T., and Martin, N. I. (2014) Small molecule inhibitors of histone acetyltransferases and deacetylases are potential drugs for inflammatory diseases. *Drug Discov. Today 19*, 654-660.
23. Chen, L. F., Fischle, W., Verdin, E., and Greene, W. C. (2001) Duration of nuclear NF-kappaB action regulated by reversible acetylation. *Science 293*, 1653-1657.
24. Van den Bosch, T., Boichenko, A., Leus, N. G., Ourailidou, M. E., Wapenaar, H., Rotili, D., Mai, A., Imhof, A., Bischoff, R., Haisma, H. J., and Dekker, F. J. (2015) The histone acetyltransferase p300 inhibitor C646 reduces pro-inflammatory gene expression and inhibits histone deacetylases. *Biochem. Pharmacol. 102*, 130-140.
25. Leus, N. G., van der Wouden, P. E., van den Bosch, T., Hooghiemstra, W. T., Ourailidou, M. E., Kistemaker, L. E., Bischoff, R., Gosens, R., Haisma, H. J., and Dekker, F. J. (2016) HDAC 3-selective inhibitor RGFP966 demonstrates anti-inflammatory properties in RAW 264.7 macrophages and mouse precision-cut lung slices by attenuating NF-κB p65 transcriptional activity. *Biochem. Pharmacol. 108*, 58-74.
26. Quivy, V., and van Lint, C. (2004) Regulation at multiple levels of NF-κB-mediated transactivation by protein acetylation. *Biochem. Pharmacol. 68*, 1221-1229.
27. Ashburner, B. P., Westerheide, S. D., and Baldwin, A. S. (2001) The p65 (RelA) subunit of NF-kappaB interacts with the histone deacetylase (HDAC) corepressors HDAC1 and HDAC2 to negatively regulate gene expression. *Mol. Cell. Biol. 21*, 7065-7077.
28. Chen, Y., Wang, H., Yoon, S. O., Xu, X., Hottiger, M. O., Svaren, J., Nave, K. A., Kim, H. A., Olson, E. N., and Lu, Q. R. (2011) HDAC-mediated deacetylation of NF-κB is critical for Schwann cell myelination. *Nat. Neurosci. 14*, 437-441.
29. Gonneaud, A., Gagné, J. M., Turgeon, N., and Asselin, C. (2014) The histone deacetylase Hdac1 regulates inflammatory signalling in intestinal epithelial cells. *J. Inflamm. (Lond). 11*, 43.
30. Chen, X., Barozzi, I., Termanini, A., Prosperini, E., Recchiuti, A., Dalli, J., Mietton, F., Matteoli, G., Hiebert, S., and Natoli, G. (2012) Requirement for the histone deacetylase Hdac3 for the inflammatory gene expression program in macrophages. *Proc. Natl. Acad. Sci. U. S. A. 109*, E2865-2874.
31. Kim, Y., Kim, K., Park, D., Lee, E., Lee, H., Lee, Y. S., Choe, J., and Jeoung, D. (2012) Histone deacetylase 3 mediates allergic skin inflammation by regulating expression of MCP1 protein. *J. Biol. Chem. 287*, 25844-25859.
32. Wagner, F. F., Lundh, M., Kaya, T., McCarren, P., Zhang, Y.-L., Chattopadhyay, S., Gale, J. P., Galbo, T., Fisher, S. L., Meier, B. C., Vetere, A., Richardson, S., Morgan, N. G., Christensen, D.

P., Gilbert, T. J., Hooker, J. M., Leroy, M., Walpita, D., Mandrup-Poulsen, T., Wagner, B. K., and Holson, E. B. (2016) An Isochemogenic Set of Inhibitors To Define the Therapeutic Potential of Histone Deacetylases in β-Cell Protection. *ACS Chem. Biol. 11*, 363-374.

33. Yardley, D. A., Ismail-Khan, R. R., Melichar, B., Lichinitser, M., Munster, P. N., Klein, P. M., Cruickshank, S., Miller, K. D., Lee, M. J., and Trepel, J. B. (2013) Randomized phase II, double-blind, placebo-controlled study of exemestane with or without entinostat in postmenopausal women with locally recurrent or metastatic estrogen receptor-positive breast cancer progressing on treatment with a nonsteroidal aromata. *J. Clin. Oncol. 31*, 2128-2135.
34. Moradei, O. M., Mallais, T. C., Frechette, S., Paquin, I., Tessier, P. E., Leit, S. M., Fournel, M., Bonfils, C., Trachy-Bourget, M. C., Liu, J., Yan, T. P., Lu, A. H., Rahil, J., Wang, J., Lefebvre, S., Li, Z., Vaisburg, A. F., and Besterman, J. M. (2007) Novel aminophenyl benzamide-type histone deacetylase inhibitors with enhanced potency and selectivity. *J. Med. Chem. 50*, 5543-5546.
35. Lu, A., Luo, H., Shi, M., Wu, G., Yuan, Y., Liu, J., and Tang, F. (2011) Design, synthesis and docking studies on benzamide derivatives as histone deacetylase inhibitors. *Bioorg. Med. Chem. Lett. 21*, 4924-4927.
36. Boissinot, M., Inman, M., Hempshall, A., James, S. R., Gill, J. H., Selby, P., Bowen, D. T., Grigg, R., and Cockerill, P. N. (2012) Induction of differentiation and apoptosis in leukaemic cell lines by the novel benzamide family histone deacetylase 2 and 3 inhibitor MI-192. *Leuk. Res. 36*, 1304-1310.
37. Velema, W. A., Szymanski, W., and Feringa, B. L. (2014) Photopharmacology: Beyond proof of principle. *J. Am. Chem. Soc. 136*, 2178–2191.
38. Lynen, F., and Ochoa, S. (1953) Enzymes of fatty acid metabolism. *Biochim. Biophys. Acta 12*, 299-314.
39. Szymanski, W., Ourailidou, M. E., Velema, W. A., Dekker, F. J., and Feringa, B. L. (2015) Light-Controlled Histone Deacetylase (HDAC) Inhibitors: Towards Photopharmacological Chemotherapy. *Chem. - A Eur. J. 21*, 16517-16524.
40. Lauffer, B. E., Mintzer, R., Fong, R., Mukund, S., Tam, C., Zilberleyb, I., Flicke, B., Ritscher, A., Fedorowicz, G., Vallero, R., Ortwine, D. F., Gunzner, J., Modrusan, Z., Neumann, L., Koth, C. M., Kaminker, J. S., Heise, C. E., and Steiner, P. (2013) Histone deacetylase (HDAC) inhibitor kinetic rate constants correlate with cellular histone acetylation but not transcription and cell viability. *J. Biol. Chem. 288*, 26926-26943.
41. Chou, C. J., Herman, D., and Gottesfeld, J. M. (2008) Pimelic diphenylamide 106 is a slow, tight-binding inhibitor of class I histone deacetylases. *J. Biol. Chem. 283*, 35402-35409.
42. Das Gupta, K., Shakespear, M. R., Iyer, A., Fairlie, D. P., and Sweet, M. J. (2016) Histone deacetylases in monocyte/macrophage development, activation and metabolism: refining HDAC targets for inflammatory and infectious diseases. *Clin. Transl. Immunol. 5*, e62.
43. Grabiec, A. M., Krausz, S., de Jager, W., Burakowski, T., Groot, D., Sanders, M. E., Prakken, B. J., Maslinski, W., Eldering, E., Tak, P. P., and Reedquist, K. A. (2010) Histone deacetylase inhibitors suppress inflammatory activation of rheumatoid arthritis patient synovial macrophages and tissue. *J. Immunol. 184*, 2718-2728.
44. Halili, M. A., Andrews, M. R., Labzin, L. I., Schroder, K., Matthias, G., Cao, C., Lovelace, E., Reid, R. C., Le, G. T., Hume, D. A., Irvine, K. M., Matthias, P., Fairlie, D. P., and Sweet, M. J. (2010) Differential effects of selective HDAC inhibitors on macrophage inflammatory responses to the Toll-like receptor 4 agonist LPS. *J. Leukoc. Biol. 87*, 1103-1114.

Supplementary information

General

Chemicals were obtained from commercial suppliers (Sigma Aldrich, Acros Organics, Axon Medchem) and used without further purification, unless stated otherwise. Aluminum sheets of Silica Gel 60 F254 were used for Thin Layer Chromatography (TLC). Spots were visualized under ultraviolet light or stained with $KMnO_4$ solution. MP Ecochrom Silica Gel 32-63 60 Å was used for flash column chromatograph. NMR spectra were recorded on a Bruker Avance 500 spectrometer (^{1}H NMR; 500 MHz, ^{13}C NMR; 125 MHz). Chemical shift values are reported in ppm (δ) relative to tetramethylsilane (TMS). Coupling constants (J) are reported in Hz with the following splitting abbreviations: s = singlet, d = doublet, t = triplet, q = quartet and m = multiplet.

Synthetic procedures

(*E*)-3 and 2-(phenyldiazenyl)aniline were synthesized as described previously.[1]

(*E*)-methyl 4-(((4-(phenyldiazenyl)phenyl)amino)methyl)benzoate (1)

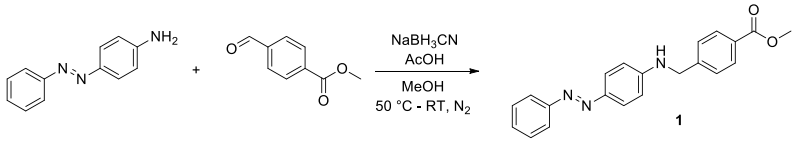

(*E*)-4-(phenyldiazenyl)aniline (0.87 g, 4.4 mmol, 1.1 eq) and methyl-4-formylbenzoate (0.70 g, 4.0 mmol, 1.0 eq) were dissolved in MeOH (7.0 mL). The mixture was heated to 50 °C and a catalytic amount of acetic acid (11 drops) was added. After 1h, the resulting mixture was cooled to room temperature and $NaBH_3CN$ (0.75 g, 12 mmol, 3.0 eq) and molecular sieves were added under nitrogen flow and stirred for 18h. After completion, the reaction was quenched with water (5.0 mL). The solvent was evaporated and the mixture was extracted with EtOAc (3 x 20 mL). The organic layer was washed with water (2 x 20 mL), dried over Mg_2SO_4 and the solvent was removed under vacuum. The crude mixture was purified by flash chromatography on silica gel (EtOAc:petroleum ether 1:6) affording **1** as an orange solid (0.93 g, 67%). R_f = 0.61 (EtOAc:petroleum ether 1:1). ^{1}H NMR (500 MHz, $CDCl_3$): δ = 8.04 (d, *J* = 8.3 Hz, 2H), 7.84-7.83 (m, 4H), 7.49-7.38 (m, 5H), 6.69 (d, *J* = 8.3 Hz, 2H), 4.65 (bs, 1H), 4.50 (s, 2H), 3.92 (s, 3H) ppm. ^{13}C NMR (125 MHz, $CDCl_3$): δ = 167.0, 153.2, 150.5, 145.2, 144.0, 130.2 (x2), 129.8, 129.5, 129.1 (x4), 127.2 (x2), 125.4, 122.4, 112.7 (x2), 52.3, 47.7 ppm.

(*E*)-4-(((4-(phenyldiazenyl)phenyl)amino)methyl)benzoic acid (2)

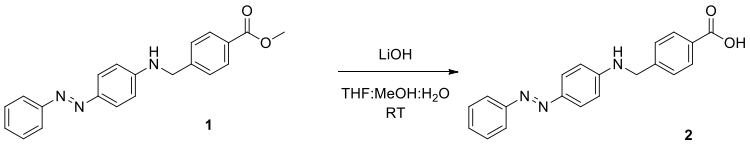

Compound **1** (0.93 g, 2.7 mmol, 1.0 eq) was dissolved in THF:MeOH (2:1) (10 mL) and a solution of LiOH (0.13 g, 5.4 mmol, 2.0 eq) in water (5.0 mL) was added at 0 °C. After 1h stirring at room temperature, another 2.0 eq of LiOH were added. After 5h stirring at room temperature, the mixture was acidified to pH 1.0 with a 4N solution of HCl and the solvents were evaporated. The residue was then dissolved in EtOAc (10 mL) and washed with water (3 x 10 mL). The organic phase was then dried over Mg_2SO_4 and evaporated under reduced pressure to afford **2** as a pale yellow solid (0.85 g, 96%). R_f = 0.22 (EtOAc:petroleum ether 1:1.2). ^{1}H NMR (500 MHz, (CD3)OD. ^{1}H NMR (500 MHz, $(CD_3)OD$): δ = 8.01 (d, *J* = 8.3 Hz, 2H), 7.77-7.73 (m, 4H), 7.50-7.45 (m, 4H), 7.39-7.36 (m, 1H), 6.71 (d, *J* = 8.3 Hz, 2H), 4.51 (s, 2H) ppm. ^{13}C NMR (125 MHz, $(CD_3)OD$): δ = 169.9, 154.4, 153.2, 146.5, 145.4, 131.0 (x2), 130.5 (x2),130.0 (x2), 128.1 (x2), 126.2 (x2), 123.0 (x2), 113.3 (x2), 61.5 ppm.

(*E*)-*tert*-butyl (2-(4-(((4-(phenyldiazenyl)phenyl)amino)methyl)benzamido) phenyl) carbamate (3)

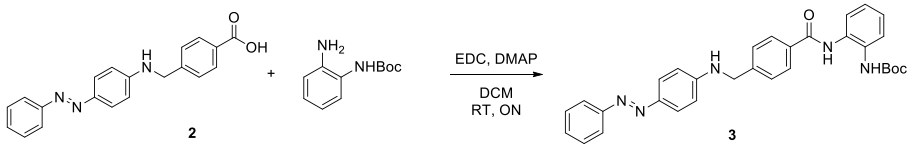

To a solution of **2** (0.33 g, 1.0 mmol, 1.0 eq) in dichloromethane (DCM) (5.0 mL) were added 4-dimethylaminopyridine (DMAP) (37 mg, 0.3 mmol, 0.3 eq) and EDC (0.23 g, 1.2 mmol, 1.2 eq) on ice. The reaction mixture was stirred for 0.5h and then *tert*-butyl (2-aminophenyl)carbamate (0.21 g, 1.0 mmol, 1.0 eq) was added and the mixture was further stirred at room temperature overnight. The solvent was evaporated and the residue was purified by flash chromatography on silica gel (EtOAc:petroleum ether 1:2) affording **3** as an orange solid (300 mg, 56%). ^{1}H NMR (500 MHz, $CDCl_3$): δ = 9.19 (s, 1H), 8.72 (s, 1H), 7.97 (d, *J* = 8.1 Hz, 2H), 7.85-7.81 (m, 4H), 7.49-7.46 (m, 4H), 7.40-7.37 (m, 1H), 7.25-7.23 (m, 2H), 7.19-7.16 (m, 1H), 6.76 (s, 1H), 6.71 (d, *J* = 8.1 Hz, 2H), 4.53 (s, 2H), 1.50 (s, 9H) ppm. ^{13}C NMR (125 MHz, $CDCl_3$): δ = 165.2, 154.9, 149.0, 148.7, 142.7, 140.1, 133.7, 131.2, 129.9, 129.8, 129.3, 129.2 (x2), 128.1 (x2), 127.6 (x2), 126.3, 126.1, 125.9 (x2), 124.7 (x2), 122.3 (x2), 120.6, 81.7, 47.7, 28.4 (x3) ppm.

(*E*)-*N*-(2-aminophenyl)-4-(((4-(phenyldiazenyl)phenyl)amino)methyl)benzamide dihydrochloride (4)

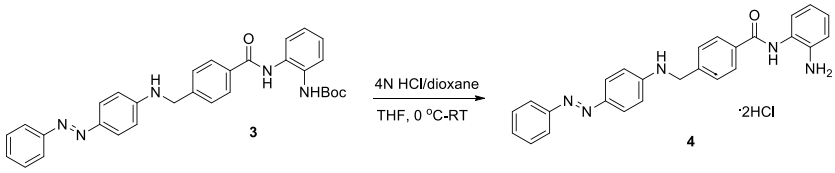

A 4N solution of HCl in dioxane (1.5 mL) was added dropwise at 0 °C to a stirred solution of **3** (46 mg, 0.1 mmol, 1.0 eq) in tetrahydrofuran (THF) (5.0 mL). After stirring for 17h at room temperature, the reaction mixture was filtered and dried under vacuum. The solid was triturated with THF and filtered to yield **4** as a purple solid (33 mg, 76%). ^{1}H NMR (500 MHz, $(CD_3)_2SO$): δ = 9.75 (s, 1H), 7.98 (d, *J* = 7.8 Hz, 2H), 7.74-7.69 (m, 4H), 7.51-7.50 (m, 4H), 7.43-7.41 (m, 3H), 7.21 (d, *J* = 7.8 Hz, 1H), 7.02-7.01 (m, 1H), 6.88 (d, *J* = 7.6 Hz, 1H), 6.72 (d, *J* = 8.6 Hz, 2H), 4.50 (s, 2H) ppm. ^{13}C NMR (125 MHz, $(CD_3)_2SO$): δ = 171.3, 165.2, 152.4, 151.8, 143.3, 143.1, 133.1, 129.6 (x2), 129.2 (x2), 128.0 (x2), 126.9 (x2), 126.7 (x2), 126.5 (x2), 125.0 (x2), 121.8 (x2), 112.1 (x2), 45.7 ppm. HRMS: $C_{26}H_{22}ON_5$ mass expected $[M+H]^+$ 422.19754, mass found 422.1973.

tert-Butyl (2-(4-formylbenzamido)phenyl)carbamate (5)

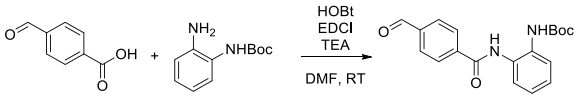

To an ice-cooled solution of 4-formylbenzoic acid (0.23 g, 1.5 mmol, 1.1 eq) in dimethylformamide (DMF) (5.0 mL) were added *N*-(3-dimethylaminopropyl)-*N*'-ethylcarbodiimide (EDCI, 0.35 g, 1.8 mmol, 1.3 eq), 1-hydroxybenzotriazole hydrate (HOBt, 0.35 g, 1.8 mmol, 1.3 eq) and trimethylamine (TEA) (0.68 mL, 4.88 mmol, 3.5 eq). After 30 min, *tert*-butyl (2-aminophenyl)carbamate (0.29 mg, 1.4 mmol, 1.0 eq) was added and the mixture was stirred at room temperature for 20h. Then, the reaction was quenched with $NaHCO_3$ (20 mL) and extracted with EtOAc (3 x 20 mL). The organic layer was washed with Na_2CO_3 and brine, dried over $MgSO_4$ and concentrated. The crude mixture was purified by flash chromatography on silica gel (EtOAc:petroleum ether 1:3) giving the pure compound **5** as a white solid (150 mg, 32%). ^{1}H NMR (500 MHz, $CDCl_3$): δ = 10.06 (s, 1H), 9.63 (bs, 1H), 8.07 (d, *J* = 8.1 Hz, 2H), 7.93 (d, *J* = 8.1 Hz, 2H), 7.71 (d, *J* = 7.9 Hz, 1H), 7.18 (d, *J* = 8.1 Hz, 1H), 7.14 (m, 1H), 7.08 (m, 1H), 1.48 (s, 9H) ppm. ^{13}C NMR (125 MHz, $CDCl_3$): δ = 191.8, 164.6, 154.9 (x2), 139.5, 138.4, 130.4, 130.1, 129.8 (x2), 128.2 (x2), 126.3, 125.9, 124.5, 81.6, 28.3 (x3) ppm.

tert-Butyl-(*E*)-(2-(4-(((3-(phenyldiazenyl)phenyl)amino)methyl)benzamido) phenyl)carbamate (6)

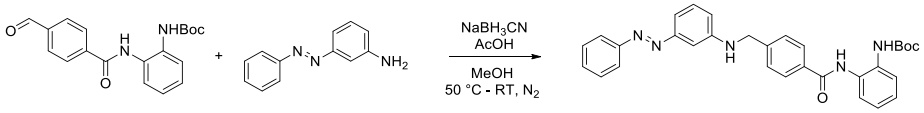

5 6

The same procedure was followed as for the synthesis of compound **1**. The crude mixture was purified by flash chromatography on silica gel (EtOAc in petroleum ether gradient elution 0-30%) affording the compound **6** as an orange solid (40 mg, 30%). ^{1}H NMR (500 MHz, $CDCl_3$): δ = 9.19 (bs, 1H), 7.94-7.88 (m, 4H), 7.72-7.71 (m, 1H), 7.51-7.48 (m, 2H), 7.45 (d, *J* = 8.2 Hz, 2H), 7.32-7.29 (m, 2H), 7.18-7.15 (m, 2H), 7.14-7.11 (m, 1H), 7.03 (t, *J* = 7.7 Hz, 1H), 6.77-6.73 (m, 1H), 6.62 (d, *J* = 8.1 Hz, 1H), 4.48 (s, 1H), 4.39 (s, 2H), 1.49 (s, 9H) ppm. ^{13}C NMR (125 MHz, $CDCl_3$): δ = 165.6, 154.7, 153.9, 152.8, 148.7, 143.6, 143.5, 133.3, 131.0, 129.9, 129.2 (x2), 127.9 (x3), 127.7 (x2), 126.1, 126.0, 125.9, 124.6, 122.9 (x2), 116.0, 113.9, 105.8, 81.4, 48.0, 28.4 (x3) ppm.

(*E*)-*N*-(2-aminophenyl)-4-(((3-(phenyldiazenyl)phenyl)amino)methyl)benzamide dihydrochloride (7)

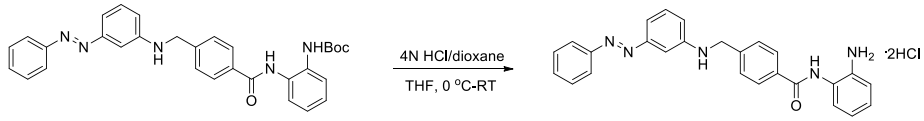

6 7

To an ice-cooled solution of **6** (40 mg, 0.08 mmol, 1.0 eq) in THF (1.0 mL) were added HCl (0.4 mL, 4N solution in dioxane). The mixture was stirred for 18h and the solvent was then removed by filtration. The solid was washed over the filter with diethyl ether to afford the desired compound **7** as an orange solid (20 mg, 55%). ^{1}H NMR (500 MHz, $(CD_3)_2SO$): δ = 10.55 (s, 1H), 10.53 (s, 1H), 8.09 (d, *J* = 8.1 Hz, 2H), 7.82 (d, *J* = 7.2 Hz, 1H), 7.64 (d, *J* = 8.1 Hz, 1H), 7.63-7.56 (m, 4H), 7.52-7.49 (m, 1H), 1.45-1.40 (m, 1H), 7.34 (m, 1H), 7.29-7.27 (m, 1H), 7.14-7.10 (m, 2H), 6.84 (d, *J* = 8.2 Hz, 1H), 6.69 (t, *J* = 7.4 Hz, 1H), 6.63 (d, *J* = 8.2 Hz, 1H), 4.48 (s, 2H) ppm. ^{13}C NMR (125 MHz, $(CD_3)_2SO$): δ = 165.5, 152.9, 151.9, 144.1, 143.4, 132.2, 131.3, 129.7, 129.5 (x2), 128.8, 128.3, 128.2 (x2), 127.3 (x2), 127.1, 126.6, 124.0, 122.4 (x2), 119.6, 115.2, 112.9, 105.6, 46.0 ppm. HRMS: $C_{26}H_{22}ON_5$ mass expected $[M+H]^+$ 422.19754, mass found 422.19721.

tert-Butyl-(*E*)-(2-(4-(((2-(phenyldiazenyl)phenyl)amino)methyl)benzamido) phenyl) carbamate (8)

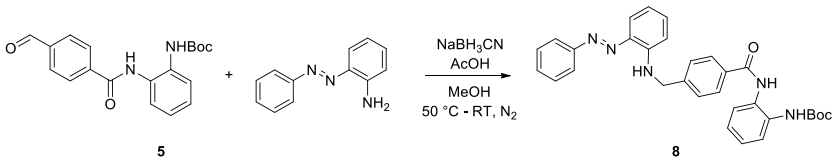

5 8

The same procedure as described for the synthesis of compound **1** was followed. The crude mixture was purified by flash chromatography on silica gel EtOAc:petroleum ether 1:3 to yield **7** as a red solid (28 mg, 37%). ^{1}H NMR (500 MHz, $CDCl_3$): δ = 9.16 (bs, 2H), 7.96 (d, *J* = 8.1 Hz, 2H), 7.91 (dd, *J* = 8.1 Hz, *J* = 1.5 Hz, 1H), 7.79 (d, *J* = 8.1 Hz, 2H), 7.50-7.47 (m, 4H), 7.42-7.39 (m, 1H), 7.24-7.22 (m, 3H), 7.17-7.14 (m, 1H), 6.83 (t, *J* = 7.5 Hz, 2H), 6.71 (d, *J* = 8.1 Hz, 1H), 4.62 (s, 2H), 3.34 (s, 1H), 1.48 (s, 9H) ppm. ^{13}C NMR (125 MHz, $CDCl_3$): δ = 165.5, 154.8, 152.9, 143.2, 143.1, 136.7, 133.7, 133.5, 132.9, 131.1, 130.8, 130.0, 129.3 (x2), 128.0 (x2), 127.3 (x2), 126.2, 126.1, 125.9, 124.6, 122.2 (x2), 116.6, 112.3, 81.6, 46.8, 28.4 (x3) ppm.

(*E*)-*N*-(2-aminophenyl)-4-(((2-(phenyldiazenyl)phenyl)amino)methyl)benzamide (9)

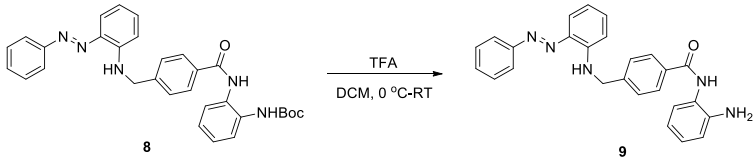

8 9

To an ice-cooled solution of **8** (30 mg, 0.06 mmol, 1.0 eq) in DCM (5.0 mL) was added trifluoroacetic acid (16 µL, 0.20 mmol, 3.5 eq). The mixture was left stirring at room temperature overnight. Then, it was washed with $NaHCO_3$ (2 x 5 mL) and Na_2CO_3 (1 x 5 mL). The organic phase was dried over Mg_2SO_4 and evaporated under reduced pressure. The residue was purified by column chromatography (EtOAc:petroleum ether 1:1) to afford **9** as a red solid (3.6 mg, 14%). ^{1}H NMR (500 MHz, $CDCl_3$): δ = 9.17 (bs, 1H), 7.91 (d, *J* = 8.1 Hz, 2H), 7.85 (s, 1H), 7.79 (d, *J* = 8.1 Hz, 2H), 7.52-7.48 (m, 4H), 7.41 (t, *J* = 7.2 Hz, 1H), 7.34 (d, *J* = 7.8 Hz, 1H), 7.24-7.22 (m, 1H), 7.10 (t, *J* = 7.4 Hz, 1H), 6.85-6.82 (m, 3H), 6.70 (d, *J* = 8.1 Hz, 1H), 4.63 (s, 2H) ppm. ^{13}C NMR (125 MHz, $CDCl_3$): δ = 168.9, 155.7, 152.9, 143.3, 143.2, 136.7, 133.3, 132.9, 130.8, 130.0, 129.3 (x2), 127.9 (x2), 127.6, 127.5 (x2), 127.4, 125.3, 122.3 (x2), 120.1, 118.7, 116.6, 112.3, 46.8 ppm. HRMS: $C_{26}H_{22}ON_5$ mass expected $[M+H]^+$ 422.19754, mass found 422.19716.

Inhibition studies

Human recombinant C-terminal His-Tag, C-terminal FLAG-tag HDAC1, C-terminal FLAG-tag HDAC2, C-terminal His-tag HDAC3/NcoR2, and C-terminal His-tag HDAC8 and HDAC6 GST-tag were purchased from BPS Bioscience. The HDAC assay substrate (Boc-Lys-(Ac)-AMC) and the HDAC assay deacetylated standard (Boc-Lys-AMC) were purchased from Bachem, Germany. The developer (Trypsin from porcine pancreas Type IX-S, lyophilized powder, 13,000-20,000 BAEE units/mg protein) and Bovine Serum Albumin (BSA) were purchased from Sigma Aldrich, The Netherlands. Endopeptidase Lys-C, *Achromobacter lyticus* was purchased from Merck Millipore and used as a developer during the monitoring of HDAC activity (release of 7-amino-4-methylcoumarin (AMC)) over the time. Reactions were conducted in black 96-well flat bottom microplates (Corning® Costar®, Corning Incorporated, NY). The fluorescence measurements were carried out in a Synergy H1 Hybrid Multi-Mode Microplate Reader (BioTek, USA) and the gain setting of the instrument was adjusted to 70, apart from HDAC8 experiments, where a gain of 100 was used. GraphPad Prism 5.0, GraphPad Software, Inc. GraphPad was used for the determination of kinetic values and of the half maximal inhibitory concentration (IC_{50}) of each inhibitor. Non-linear regression was used for data fitting.

Measurement of IC_{50} values of compounds 4, 7, and 9 on HDACs 1-3 and 8

The HDAC inhibition assays were performed as described previously at steady state conditions.[1] Non-linear regression was used for data fitting. The K_i values were calculated from Cheng-Prusoff equation: $K_i = IC_{50}/(1+[S]/K_m)$. There was observed no inhibition against HDAC8.

Measurement of kinetic parameters k_{on} and k_{off} on HDAC1-3

The kinetic parameters were determined as described previously.[2] A series of inhibition progression curves for HDACs 1-3, at different concentrations of each inhibitor, were generated by adding 47/132/55 ng of HDAC1, 2 and 3 respectively into reaction mixtures containing a final concentration of 125/200/80 μM of Boc-Lys(Ac)-AMC (for each HDAC accordingly) and 2 mU of Lys-C peptidase developer. Positive control (no inhibitor) and blank (no enzyme) wells were also set up. The experiments were performed in triplicate. The release of fluorescent 7-amino-4-methylcoumarin (AMC) was monitored continuously for 60-90 min at ambient temperature and gain 70. The reaction rates (every 2 min intervals) were calculated and the ln values of the rates were plotted versus the time. The slope of the resulting linear graphs, corresponding to the k_{obs}, was plotted versus the inhibitor concentration. The k_{on} values were then calculated according to the following equation:

$$k_{obs} = k_{off} + k_{on}[I](1+[S]/K_m)$$

0.8/2.3/1.1 µM of HDACs 1-3 were incubated with an inhibitor concentration varying from 2-16 µM (according to IC_{50} values) for 1h at room temperature. Positive control (no inhibitor) mixtures were also set up. 1 µL of each mixture was diluted into a total reaction volume of 100 µL containing a final concentration of 125/200/80 µM of Boc-Lys(Ac)-AMC (for each HDAC accordingly) and 2 mU of Lys-C peptidase developer. The experiments were performed in triplicate. The release of fluorescent AMC was monitored continuously for 60-90 min at ambient temperature and gain 70. The reaction rates (every 2 min intervals) were calculated and the difference between the rate of the positive control and the inhibitor wells was plotted versus the reaction time in GraphPad Prism 5.0. The data were fit using non-linear regression-dissociation - one phase exponential decay model.

Pharmacological studies

Cell culture

Murine RAW264.7 and RAW blue macrophages were purchased from the American Type Culture Collection (ATCC; Wesel, Germany) and cultured in plastic tissue culture plates or flasks (Costar Europe, Badhoevedorp, The Netherlands) at 37 °C under 5% CO_2/95% air in Dulbecco's Modification of Eagle's Medium (DMEM) containing GlutaMAX™ (Gibco® by Life Technologies, Bleiswijk, The Netherlands) supplemented with 10% (v/v) heat inactivated fetal bovine serum (FBS; Invitrogen, Breda, The Netherlands), 2 mM additional GlutaMAXTM (Gibco® by Life Technologies), 100 U/mL penicillin (Gibco® by Life Technologies) and 100 µg/mL streptomycin (Gibco® by Life Technologies). 15 and 50 mL centrifuge tubes, serological pipettes and cell culture flasks were purchased from Greiner bio-one, The Netherlands.

Cell viability assays

The toxicity of the HDACi was examined as described previously.[3] RAW264.7 macrophages were seeded to afford 25000 cells/cm^2. The next day, medium was replaced with fresh medium containing the respective HDACi (pre-heated DMSO stock solutions) at the indicated concentrations. After 16h incubation, cells were stimulated with 10 ng/mL lipopolysaccharide (LPS, *Escherichia coli*, serotype 0111:B4; Sigma-Aldrich, Zwijndrecht, the Netherlands) and 10 ng/mL interferon gamma (IFN, #315-05; PeproTech, Hamburg, Germany) for the last 4h of the experiment. 20 µL of CellTiter 96 Aqueous One Solution reagent (CellTiter 96 Aqueous One Solution Cell Proliferation Assay Kit, Promega, the Netherlands) was added to each well and incubated at 37 °C for 1h in the dark. The absorbance at 490 nm was measured using a Synergy H1 plate reader. LPS/IFNγ-stimulated cells non-treated with HDACi were set as 100% (control). DMSO did not affect the cells' viability.

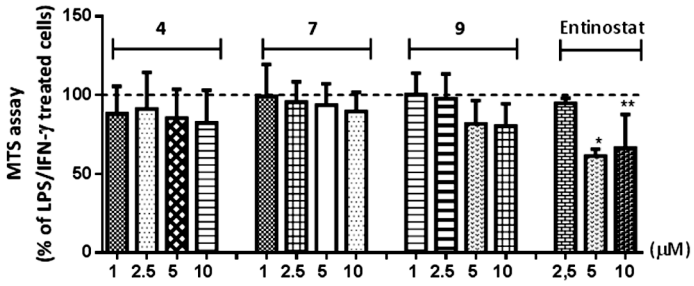

Figure S1. RAW264.7 cellular viability assessment after 16h incubation with the respective HDACi followed by treatment with the inflammatory stimuli LPS/IFNγ for additional 4h.

NF-κB reporter gene assay

QUANTI-blue assay was used to monitor the NF-κB promoter activity.[3] Raw blue cells were treated with the HDACi at the appropriate concentrations and further stimulated as described above. The secretion of SEAP into the medium was determined using the QUANTI-Blue™ detection medium (InvivoGen) according to the manufacturer's instructions. The absorbance at 630 nm was measured and the results were plotted as % of the control.

Nuclear translocation of NF-κB p65

Confocal laser scanning microscopy was used to investigate the effect of HDACi on nuclear translocation of NF-κB p65 by immunofluorescence as reported previously.[3] RAW264.7 cells were incubated with the 1 μM of each compound for 20h and stimulated at the last hour as described above.

Gene expression analysis by RT-q-PCR

A previously described method was followed.[3] RAW264.7 cells were incubated with the compounds and stimulated as described above. The primers for TNFα (Mm00443258_m1), IL-1β (Mm00434228_m1), IL-6 (Mm00446190_m1), iNOS (Mm00440502_m1) IL-12b (Mm00434174_m1) and GAPDH (Mm99999915_g1) were purchased as Assay-on-Demand (Applied Biosystems).

Supplementary references

1. Szymanski, W., Ourailidou, M. E., Velema, W. A., Dekker, F. J., and Feringa, B. L. (2015) Light-controlled Histone Deacetylase (HDAC) Inhibitors: Towards Photopharmacological Chemotherapy. *Chem. - A Eur. J. 21*, 16517-16524.
2. Chou, C. J., Herman, D., and Gottesfeld, J. M. (2008) Pimelic diphenylamide 106 is a slow, tight-binding inhibitor of class I histone deacetylases. *J. Biol. Chem. 283*, 35402-35409.

3. Leus, N. G., van der Wouden, P. E., van den Bosch, T., Hooghiemstra, W. T., Ourailidou, M. E., Kistemaker, L. E., Bischoff, R., Gosens, R., Haisma, H. J., and Dekker, F. J. (2016) HDAC 3-selective inhibitor RGFP966 demonstrates anti-inflammatory properties in RAW 264.7 macrophages and mouse precision-cut lung slices by attenuating NF-κB p65 transcriptional activity. *Biochem. Pharmacol. 108*, 58-74.